

HETÉNYI'S ELASTIC QUARTER SPACE PROBLEM REVISITED

L. M. KEER, J. C. LEE and T. MURA

The Technological Institute, Northwestern University, Evanston, IL 60201, U.S.A.

(Received 19 July 1982; in revised form 27 September 1982)

Abstract—Transform methods are used to solve the problem of an elastic quarter space subjected to tractions on its surface. The present analysis uses the reflection principle to formulate problem as the solution of unknown residual surface tractions. A Fourier transform is taken in the direction of the edge of the quarter space. The problem is thereby reduced to decouplable integral equations, which are similar to those for the elastic quarter plane. Field quantities are obtained by performing the appropriate inverse transforms and the present results are compared with those of Hetényi for the normally loaded case. Additional results are given for the cases of tangential surface loading.

INTRODUCTION

The problem of the elastic quarter space subjected to tractions on its surface is one that has had considerable interest. The case for normal loading was first investigated by Hetényi[1], who used the method of reflection and iteration of the reflected solutions to obtain a result having acceptable accuracy. His method was based upon his solution to the elastic quarter plane given earlier[2]. The method of reflection is a simple and effective numerical technique; however, it does have the drawback that the accuracy near singular points and corners may become degraded. Furthermore, if the stress decay is not rapid, then this scheme can prove to be computationally costly. Gerber, a student of Hetényi's, used the algorithm to consider the contact problem for a square indenter on an elastic quarter space[3]. A limitation of Gerber's solution was that the indenter was constrained from approaching too close to the edge of the quarter space.

Recently, Kupradze *et al.*[4], solved some problems for the quarter space through the use of potential theory. These problems included thermal effects with various boundary conditions on one face; however, on the other face either the tangential components of displacement, a normal component of stress or a normal component of displacement, tangential component of stress had to be prescribed. Numerical results were not provided.

In the present analysis, the problem is formulated by applying a Fourier transform upon the loading and the potentials in the direction of the edge of the quarter space. This effectively reduces the problem to two decouplable integral equations (having the transform variable as a parameter), which are similar to those for the elastic quarter plane (see, e.g. Sneddon[5]). In certain loading cases the unknown quantities have logarithmic singularities which can be separated from the regular part. The part that is singular is represented by a modified Bessel function of the second kind, $K_0(x)$, where the coefficient, which can be explicitly expressed for Poisson's ratio $1/2$, is included as one of the unknowns. Once the integral equations are solved, the stress and displacement components are calculated in terms of these quantities.

GENERAL THEORY

The method of solution will be somewhat analogous in form to that employed by Hetényi[1]; however, the details of the solution will make use of integral transform techniques. If normal tractions are applied on the surface $z = 0$ of the half space $z \geq 0$, then the stress components can be expressed by the Boussinesq type potential function as†

$$\sigma_{xx} = 2\nu \frac{\partial^2 \psi}{\partial z^2} - (1 - 2\nu) \frac{\partial^2 \psi}{\partial x^2} - z \frac{\partial^3 \psi}{\partial x^2 \partial z}, \quad (1)$$

†We note that the Boussinesq solution in eqn (1)–(7) has been shown to be complete *only* for axisymmetric problems (and in bounded domain)[5]. This lack of completeness of the potential function used is acknowledged; however, the reader can be assured that the results appear to satisfy all physical requirements.

$$\sigma_{yy} = 2\nu \frac{\partial^2 \psi}{\partial z^2} - (1-2\nu) \frac{\partial^2 \psi}{\partial y^2} - z \frac{\partial^3 \psi}{\partial y^2 \partial z}, \quad (2)$$

$$\sigma_{zz} = \frac{\partial^2 \psi}{\partial z^2} - z \frac{\partial^3 \psi}{\partial z^3}, \quad (3)$$

$$\sigma_{xy} = -(1-2\nu) \frac{\partial^2 \psi}{\partial x \partial y} - z \frac{\partial^3 \psi}{\partial x \partial y \partial z}, \quad (4)$$

$$\sigma_{xz} = -z \frac{\partial^3 \psi}{\partial x \partial z^2}, \quad (5)$$

$$\sigma_{yz} = -z \frac{\partial^3 \psi}{\partial y \partial z^2}, \quad (6)$$

where

$$\nabla^2 \psi = 0 \quad (7)$$

and ν is Poisson's ratio. If the normal traction is symmetric with respect to the y - z plane (see Fig. 1), then

$$\psi = -\frac{1}{\pi^2} \int_0^\infty \int_{-\infty}^\infty \frac{A(\xi, \eta)}{\xi^2 + \eta^2} \exp(-z\sqrt{\xi^2 + \eta^2}) \cos(\xi x) \exp(-i y \eta) d\eta d\xi,$$

$$z > 0, x > 0, -\infty < y < \infty,$$

satisfies eqn (7). Similarly, the stress components due to normal traction on the surface $x = 0$ can be written in terms of the potential function, symmetric with respect to the x - y plane, given as

$$\chi = -\frac{1}{\pi^2} \int_0^\infty \int_{-\infty}^\infty \frac{B(\xi, \eta)}{\sqrt{\xi^2 + \eta^2}} \exp(-x\sqrt{\xi^2 + \eta^2}) \cos(\xi z) \exp(-i y \eta) d\eta d\xi.$$

The stress components are given by eqns (1)–(6) with x and z interchanged and ψ replaced by χ . By use of a simple superposition involving the two sets of stress components, the solution that

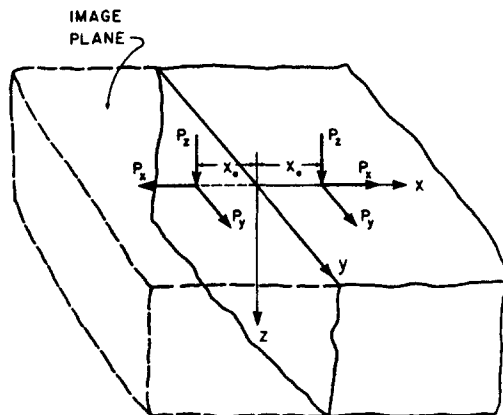


Fig. 1. Geometry and coordinate system for quarter space under normal loading, tangential loading perpendicular to the edge and tangential loading parallel to the edge.

is appropriate to the positive quadrant yields the following:

$$\begin{aligned} \sigma_{xx}(x, y, z) = & -\frac{1}{\pi^2} \int_0^\infty \int_{-\infty}^\infty A(\xi, \eta) \left[1 - (1 - 2\nu) \frac{\eta^2}{\xi^2 + \eta^2} - \frac{z\xi^2}{\sqrt{(\xi^2 + \eta^2)}} \right] \exp(-z\sqrt{(\xi^2 + \eta^2)}) \\ & \times \cos(\xi x) \exp(-iy\eta) d\eta d\xi - \frac{1}{\pi^2} \int_0^\infty \int_{-\infty}^\infty B(\xi, \eta) [1 + x\sqrt{(\xi^2 + \eta^2)}] \\ & \times \exp(-x\sqrt{(\xi^2 + \eta^2)}) \cos(z\xi) \exp(-iy\eta) d\eta d\xi, \end{aligned} \tag{8}$$

$$\begin{aligned} \sigma_{zz}(x, y, z) = & -\frac{1}{\pi^2} \int_0^\infty \int_{-\infty}^\infty A(\xi, \eta) [1 + z\sqrt{(\xi^2 + \eta^2)}] \exp(-z\sqrt{(\xi^2 + \eta^2)}) \cos(\xi x) \\ & \times \exp(-iy\eta) d\eta d\xi - \frac{1}{\pi^2} \int_0^\infty \int_{-\infty}^\infty B(\xi, \eta) \left[1 - (1 - 2\nu) \frac{\eta^2}{\xi^2 + \eta^2} - \frac{x\xi^2}{\sqrt{(\xi^2 + \eta^2)}} \right] \\ & \times \exp(-x\sqrt{(\xi^2 + \eta^2)}) \cos(\xi z) \exp(-iy\eta) d\eta d\xi \end{aligned} \tag{9}$$

where it is assumed that the quadrant is loaded *only* by normal stresses. It is clear from the form given to eqns (8) and (9) that the superposition solutions employed are formed by symmetry to automatically cancel the shear stresses on these planes. This is essentially the superposition idea that was used by Hetényi.

If on the boundary we have

$$\sigma_{zz}(x, y, 0) = -f(x, y) \tag{10}$$

$$\sigma_{xx}(0, y, z) = -g(y, z) \tag{11}$$

then the following integral equations for the Fourier transforms $A(\xi, \eta)$ and $B(\xi, \eta)$ are obtained:

$$\begin{aligned} \frac{1}{\pi^2} \int_0^\infty \int_{-\infty}^\infty A(\xi, \eta) \cos(\xi x) \exp(-iy\eta) d\eta d\xi + \frac{1}{\pi^2} \int_0^\infty \int_{-\infty}^\infty B(\xi, \eta) \left[1 - (1 - 2\nu) \frac{\eta^2}{\xi^2 + \eta^2} \right. \\ \left. - \frac{x\xi^2}{\sqrt{(\xi^2 + \eta^2)}} \right] \exp(-x\sqrt{(\xi^2 + \eta^2)}) \exp(-iy\eta) d\eta d\xi = f(x, y), 0 < x < \infty, -\infty < y < \infty \end{aligned} \tag{12}$$

$$\begin{aligned} \frac{1}{\pi^2} \int_0^\infty \int_{-\infty}^\infty A(\xi, \eta) \left[1 - (1 - 2\nu) \frac{\eta^2}{\xi^2 + \eta^2} - \frac{z\xi^2}{\sqrt{(\xi^2 + \eta^2)}} \right] \exp(-z\sqrt{(\xi^2 + \eta^2)}) \exp(-iy\eta) d\eta d\xi \\ + \frac{1}{\pi^2} \int_0^\infty \int_{-\infty}^\infty B(\xi, \eta) \cos(\xi z) \exp(-iy\eta) d\eta d\xi = g(y, z), 0 < z < \infty, -\infty < y < \infty. \end{aligned} \tag{13}$$

Next, we suppose that the Fourier transforms with respect to y of $f(x, y)$ and $g(y, z)$ exist and are given as

$$\hat{f}(x, \eta) = \int_{-\infty}^\infty f(x, y) \exp(iy\eta) dy, \tag{14}$$

$$\hat{g}(z, \eta) = \int_{-\infty}^\infty g(y, z) \exp(iy\eta) dy. \tag{15}$$

By use of $\int_{-\infty}^\infty \exp\{iy(\eta - \eta')\} dy = 2\pi\delta(\eta - \eta')$, where δ is Dirac's delta function, we take the Fourier transforms with respect to y of eqns (12), (13) to obtain the following integral equations

in terms of x and the transform variable η :

$$\frac{2}{\pi} \int_0^\infty A(\xi, \eta) \cos(\xi x) d\xi + \frac{2}{\pi} \int_0^\infty B(\xi, \eta) \left[1 - (1-2\nu) \frac{\eta^2}{\xi^2 + \eta^2} - \frac{x\xi^2}{\sqrt{(\xi^2 + \eta^2)}} \right] \exp(-x\sqrt{(\xi^2 + \eta^2)}) d\xi = \hat{f}(x, \eta), \quad 0 < x < \infty, \quad (16)$$

$$\frac{2}{\pi} \int_0^\infty A(\xi, \eta) \left[1 - (1-2\nu) \frac{\eta^2}{\xi^2 + \eta^2} - \frac{z\xi^2}{\sqrt{(\xi^2 + \eta^2)}} \right] \exp(-z\sqrt{(\xi^2 + \eta^2)}) d\xi + \frac{2}{\pi} \int_0^\infty B(\xi, \eta) \cos(z\xi) d\xi = \hat{g}(z, \eta), \quad 0 < z < \infty. \quad (17)$$

It is convenient at this point to define $A(\xi, \eta)$ and $B(\xi, \eta)$ in terms of cosine transforms as

$$A(\xi, \eta) = \int_0^\infty \hat{p}(x, \eta) \cos(x\xi) dx, \quad (18)$$

$$B(\xi, \eta) = \int_0^\infty \hat{q}(z, \eta) \cos(z\xi) dz. \quad (19)$$

If the definitions in eqns (18) and (19) are used and Parseval's theorem is applied to eqns (16) and (17), then

$$\hat{p}(x, \eta) + \frac{2}{\pi} \int_0^\infty \hat{q}(\zeta, \eta) \left[\frac{\eta^2 x \zeta^2}{x^2 + \zeta^2} K_2(\eta\sqrt{(x^2 + \zeta^2)}) - (1-2\nu) \int_0^\infty \frac{\eta^2}{u^2 + \eta^2} \times \exp(-x\sqrt{(u^2 + \eta^2)}) \cos(u\zeta) du \right] d\zeta = \hat{f}(x, \eta), \quad 0 < x < \infty, \quad (20)$$

$$\hat{q}(z, \eta) + \frac{2}{\pi} \int_0^\infty \hat{p}(\zeta, \eta) \left[\frac{\eta^2 z \zeta^2}{z^2 + \zeta^2} K_2(\eta\sqrt{(z^2 + \zeta^2)}) - (1-2\nu) \int_0^\infty \frac{\eta^2}{u^2 + \eta^2} \times \exp(-z\sqrt{(u^2 + \eta^2)}) \cos(u\zeta) du \right] d\zeta = \hat{g}(z, \eta), \quad 0 < z < \infty, \quad (21)$$

where $K_2(s)$ is a modified Bessel function of the second kind and the integral in the kernel can be expressed in the form

$$\int_0^\infty \frac{\eta^2}{u^2 + \eta^2} \exp(-x\sqrt{(u^2 + \eta^2)}) \cos(u\zeta) du = \frac{\pi}{2} \eta \exp(-\eta\zeta) - \int_0^x \eta^2 K_0(\eta\sqrt{(s^2 + \zeta^2)}) ds. \quad (22)$$

By application of the inverse Fourier transform in η and the convolution theorem, we obtain

$$p(x, y) + \frac{3}{\pi} \int_0^\infty \int_{-x}^x q(\eta, \zeta) \left\{ \frac{x\zeta^2}{R^3} - \frac{(1-2\nu)}{3} \left[\frac{x}{R^3} - \frac{1}{R(R+x)} \left\{ 1 - \frac{\zeta^2}{R(R+x)} - \frac{\zeta^2}{R^2} \right\} \right] \right\} d\eta d\zeta = f(x, y) \quad (23)$$

where

$$R^2 = x^2 + \zeta^2 + (y - \eta)^2$$

$$q(y, z) + \frac{3}{\pi} \int_0^\infty \int_{-\infty}^\infty p(\zeta, \eta) \left\{ \frac{z\zeta^2}{R^3} - \frac{(1-2\nu)}{3} \left[\frac{z}{R^3} - \frac{1}{R(R+z)} \left\{ 1 - \frac{\zeta^2}{R(R+z)} - \frac{\zeta^2}{R^2} \right\} \right] \right\} d\eta d\zeta = g(y, z) \quad (24)$$

where

$$R^2 = z^2 + \zeta^2 + (y - \eta)^2.$$

Here, we note that

$$p(x, y) = \frac{1}{2\pi} \int_{-\infty}^{\infty} \hat{p}(x, \eta) \exp(-iy\eta) d\eta, \tag{25}$$

$$q(y, z) = \frac{1}{2\pi} \int_{-\infty}^{\infty} \hat{q}(z, \eta) \exp(-iy\eta) d\eta \tag{26}$$

are the surface tractions on the plane $z = 0, x = 0$, respectively. Equations (23) and (24) are the ones solved by Hetényi using the reflection method.

Instead of solving eqns (23) and (24), we will focus on the solution to eqns (20) and (21), which are analogous to the equations that occur for the quarter plane problem (see, e.g. Sneddon[6]). Although these equations contain the transform variable η as a parameter, we will solve the quarter plane problem explicitly in terms of the transform variable and later perform the inverse transform. To decouple eqns (20), (21) let

$$\phi_1(x, \eta) = \hat{p}(x, \eta) - \hat{q}(x, \eta) \tag{27}$$

$$\phi_2(x, \eta) = \hat{p}(x, \eta) + \hat{q}(x, \eta). \tag{28}$$

Then, eqns (20), (21) become

$$\phi_1(x, \eta) - \int_0^{\infty} \phi_1(\xi, \eta) K(x, \xi; \eta) d\xi = \hat{f}(x, \eta) - \hat{g}(x, \eta) \tag{29}$$

$$\phi_2(x, \eta) + \int_0^{\infty} \phi_2(\xi, \eta) K(x, \xi; \eta) d\xi = \hat{f}(x, \eta) + \hat{g}(x, \eta) \tag{30}$$

where

$$K(x, \xi; \eta) = \frac{2}{\pi} \left\{ \frac{\eta^2 x \xi^2}{x^2 + \xi^2} K_2(\eta \sqrt{x^2 + \xi^2}) - (1 - 2\nu) \int_0^{\infty} \frac{\eta^2}{u^2 + \eta^2} \exp(-x \sqrt{u^2 + \eta^2}) \cos(u\xi) du \right\}. \tag{31}$$

For $\eta \rightarrow 0$ the kernel $K(x, \xi, \eta)$ can be written in the form

$$K(x, \xi; 0) = \frac{4}{\pi} \frac{x \xi^2}{(x^2 + \xi^2)^2} \tag{32}$$

and the resulting equations are immediately recognized as those for the quarter plane[6].

The behavior of $\phi_1(x, 0)$ or $\hat{p}(x, 0)$ and $\hat{q}(x, 0)$ near the edge is dependent on the functions \hat{f} and \hat{g} . If we denote the Mellin transform of $\phi_1(x, 0) = \phi_1(x)$ by $\phi_1^*(s)$ so that

$$\phi_1^*(s) = \int_0^{\infty} \phi_1(x) x^{s-1} dx \tag{33}$$

then by taking the Mellin transform of both sides of eqn (29) and making use of the convolution theorem, we see that the solution of eqn (29) may be written in the form

$$\phi_1(x) = \frac{1}{2\pi i} \int_{c-i\infty}^{c+i\infty} \frac{\cos(\pi s/2) \int_0^{\infty} [\hat{f}(x, 0) - \hat{g}(x, 0)] x^{s-1} dx}{(s-1) + \cos(\pi s/2)} x^{-s} ds \tag{34}$$

where $0 < c < 1$. If $f(x, 0) - g(x, 0)$ does not vanish as $x \rightarrow 0$, then it is obvious that there are

double poles at $s = 0$. This shows that a logarithmic singularity appears near the edge (see, e.g. Dundurs and Lee[7]). The deformation near the edge is well approximated by plane strain; therefore, for every transformed variable η , the logarithmic singularity occurs for $\phi_1(x, \eta)$ in eqn (29) under any type of regular loading.

In order to make the solution more accurate, decompose $\phi_1(x, \eta)$ into two parts as follows:

$$\phi_1(x, \eta) = a(\eta)K_0(x) + \phi(x, \eta) \tag{35}$$

where $\phi(x, \eta)$ is finite everywhere and $K_0(s)$ is a modified Bessel function of the second kind, which behaves asymptotically logarithmic for small argument. By substituting $\phi_1(x, \eta)$ into eqn (29), we get

$$\phi(x, \eta) - \int_0^\infty \phi(\xi, \eta)K(x, \xi; \eta) d\xi + a(\eta)\left[K_0(x) - \int_0^\infty K_0(\xi)K(x, \xi; \eta) d\xi\right] = \hat{f}(x, \eta) - \hat{g}(x, \eta) \tag{36}$$

where $a(\eta)$ is the other unknown quantity that can be obtained by an additional equation as follows. Since $\phi(x, \eta)$ is finite everywhere, let $x \rightarrow 0$ in eqn (36) and use the properties:

$$\lim_{x \rightarrow 0} \frac{2}{\pi} \int_0^\infty \phi(\xi) \frac{\eta^2 x \xi^2}{x^2 + \xi^2} K_2(\eta\sqrt{x^2 + \xi^2}) d\xi = \phi(0), \tag{37}$$

$$\lim_{x \rightarrow 0} \frac{2}{\pi} \int_0^\infty K_0(\xi) \left[\int_0^\infty \frac{\eta^2}{u^2 + \eta^2} \exp(-x\sqrt{u^2 + \eta^2}) \cos(u\xi) du \right] d\xi = \eta \cos^{-1}(\eta/\sqrt{1 - \eta^2}) \tag{38}$$

$$\frac{2}{\pi} \int_0^\infty \frac{\eta^2 x \xi^2}{x^2 + \xi^2} K_2(\eta\sqrt{x^2 + \xi^2}) K_0(\xi) d\xi = K_0(x) - 1 + O(x) \text{ as } x \rightarrow 0. \tag{39}$$

We then find that

$$(1 - 2\nu) \int_0^\infty \eta \exp(-\eta\xi)\phi(\xi, \eta) d\xi + a(\eta)\left[1 + (1 - 2\nu) \frac{\eta \cos^{-1}(\eta)}{\sqrt{1 - \eta^2}}\right] = \hat{f}(0, \eta) - \hat{g}(0, \eta) \tag{40}$$

and the problem is reduced to solving eqns (30), (36) and (40).

When Poisson's ratio $\nu = 1/2$, the equations take the simpler form given next:

$$\begin{aligned} \phi(x, \eta) - \frac{2}{\pi} \int_0^\infty \frac{\eta^2 x \xi^2}{x^2 + \xi^2} K_2(\eta\sqrt{x^2 + \xi^2})\phi(\xi, \eta) d\xi + a(\eta)\left\{K_0(x) - \frac{2}{\pi} \int_0^\infty \frac{\eta^2 x \xi^2}{x^2 + \xi^2} \right. \\ \left. \times K_2(\eta\sqrt{x^2 + \xi^2})K_0(\xi) d\xi\right\} = \hat{f}(x, \eta) - \hat{g}(x, \eta), \end{aligned} \tag{41}$$

$$\phi_2(x, \eta) + \frac{2}{\pi} \int_0^\infty \frac{\eta^2 x \xi^2}{x^2 + \xi^2} K_2(\eta\sqrt{x^2 + \xi^2})\phi_2(\xi, \eta) d\xi = \hat{f}(x, \eta) + \hat{g}(x, \eta) \tag{42}$$

and

$$a(\eta) = \hat{f}(0, \eta) - \hat{g}(0, \eta). \tag{43}$$

For this case the magnitude of the singularity coefficient is governed by the difference of the loadings between the top and side planes near the edge.

EXAMPLES

The technique described in the previous section is now applied to the solution of point force problems for the elastic quarter space. Three problems are considered as follows: concentrated normal load applied to top surface, concentrated shear load applied to top surface perpendicular to the edge, and concentrated shear load applied to top surface and parallel to edge.

Concentrated normal load applied to top surface (Hetényi's problem)

For a concentrated load P_z applied at the point $(x_0, 0, 0)$ we place an image load of equal magnitude at $(-x_0, 0, 0)$. This superposition clears the y - z plane of shear stresses and leaves a normal stress $g(y, z)$, having the following distribution:

$$g(y, z) = -\frac{3P_z}{2\pi} \frac{zx_0^2}{R^3} + \frac{(1-2\nu)P_z}{2\pi} \left\{ \frac{z}{R^3} - \frac{1}{R(R+z)} \left[1 - \frac{x_0^2}{R(R+z)} - \frac{x_0^2}{R^2} \right] \right\}, \tag{44}$$

where

$$R^2 = x_0^2 + y^2 + z^2. \tag{45}$$

Since it is intended to use the method outlined in the previous section, the Fourier transform with respect to y is taken, giving the following result:

$$\hat{g}(z, \eta) = -\frac{2P_z}{\pi} \frac{\eta^2 zx_0^2}{z^2 + x_0^2} K_2(\eta\sqrt{z^2 + x_0^2}) + (1-2\nu)P_z \left[\eta \exp(-\eta x_0) - \frac{2}{\pi} \int_0^z \eta^2 K_0(\eta\sqrt{s^2 + x_0^2}) ds \right]. \tag{46}$$

For $\eta = 0$, $\hat{g}(z, 0) \rightarrow 0$ as $z \rightarrow 0$. The equivalent surface tractions will be finite everywhere [1].

Concentrated shear load perpendicular to the surface

For a concentrated load P_x applied at the point $(x_0, 0, 0)$ we place an image load as shown at the point $(-x_0, 0, 0)$. For this case the distributed load on the yz -plane is

$$g(y, z) = \frac{P_x x_0}{2\pi R^3} \left\{ \frac{3x_0^2}{R^2} - \frac{1-2\nu}{(R+z)^2} \left[3R^2 - y^2 - \frac{2Ry^2}{R+z} \right] \right\}. \tag{47}$$

The corresponding surface tractions p and q will, as in the previous case, be symmetric with respect to the x - z plane. The Fourier transform of $g(y, z)$ is

$$\hat{g}(z, \eta) = \frac{2}{\pi} P_x \frac{\eta^2 x_0^3}{z^2 + x_0^2} K_2(\eta\sqrt{z^2 + x_0^2}) - (1-2\nu)P_x \frac{2}{\pi} \left\{ \eta^2 K_0(\eta\sqrt{z^2 + x_0^2}) - \frac{\pi}{2} z \eta^2 \exp(-\eta x_0) + z \int_0^z \frac{\eta^3}{\sqrt{(s^2 + x_0^2)}} K_1(\eta\sqrt{s^2 + x_0^2}) ds \right\}. \tag{48}$$

For $\eta = 0$, $\hat{g}(z, 0) \rightarrow 4/\pi$ as $z \rightarrow 0$ and a logarithmic singularity will appear at the edge.

Concentrated shear load applied to top surface and parallel to edge

For this case the distributed load on the y - z plane is, after application of image load for P_y , as follows:

$$g(y, z) = -\frac{P_y}{2\pi} \frac{y}{R^3} \left\{ \frac{3x_0^2}{R^2} - \frac{1-2\nu}{(R+z)^2} \left[3R^2 - y^2 - \frac{2Ry^2}{R+z} \right] \right\}. \tag{49}$$

Here, since $g(y, z) = -g(y, -z)$, the tractions p and q will be antisymmetric with respect to the x - z plane. The Fourier transform of $g(y, z)$ is

$$\hat{g}(z, \eta) = i \frac{2P_y}{\pi} \left\{ \frac{\eta^2 x_0^2}{\sqrt{(z^2 + x_0^2)}} K_1(\eta\sqrt{z^2 + x_0^2}) - (1-2\nu) \left[\eta^3 z \int_0^z K_0(\eta\sqrt{s^2 + x_0^2}) ds - \frac{\pi}{2} \eta^2 x_0 \exp(-\eta x_0) + \eta^2 \sqrt{(z^2 + x_0^2)} K_1(\eta\sqrt{(z^2 + x_0^2)}) \right] \right\} \tag{50}$$

and the p and q functions will also be singular near the edge.

NUMERICAL RESULTS

In solving eqns (30), (36) and (40), a 20 point Gauss-Legendre integration scheme is used. The infinite domain is transformed into the interval $(-1, 1)$ by the transformation $\xi = \tan(\pi(1 + u)/4)$, which provides a finer mesh near the corner of the quarter space, where (1) the transforms \hat{p} and \hat{q} are functions that vary rapidly in the x and z directions and (2) the first term in eqns (30) and (36) has a high peak when both x and ξ are small. To avoid the high peak in the kernel, some modification is necessary (e.g. see Baker [7]). We write

$$\int_a^b p(\xi)K(x, \xi) d\xi = \int_a^b [p(\xi) - p(x)]K(x, \xi) d\xi + p(x) \int_a^b K(x, \xi) d\xi$$

where the first term in the right-hand side is smoother and the integral in the second term may have closed form. In the numerical values to be presented here the values of the respective functions in the x and z directions are given at such x_i and ξ_i abscissa nodes.

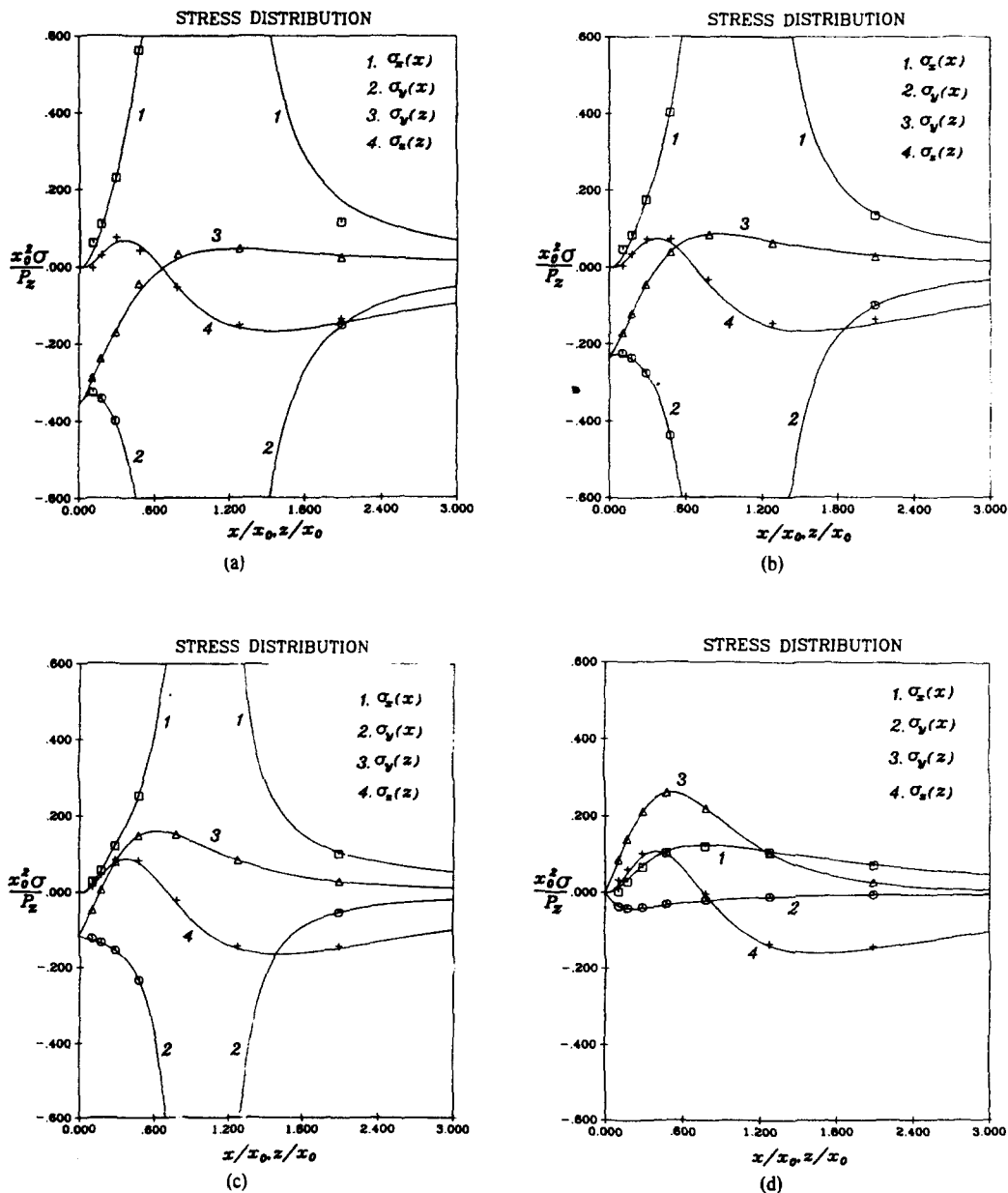


Fig. 2. Stress distributions along the crest ($y = 0$) for the quarter space under normal loading (a) $\nu = 0$; (b) $\nu = 1/6$; (c) $\nu = 1/3$; (d) $\nu = 1/2$ (symbolic line: Hetényi's result; solid line: present method).

To evaluate the stress components along the crest ($y = 0$), where the maximum stress values will occur, the inverse Fourier exponential transform can, owing to symmetry, be reduced to the Fourier cosine transform. In the numerical calculation of the inverse Fourier cosine transforms for the transformed stress components, 26 point Gaussian quadrature, in which 11 points Radau Gaussian quadrature and 15 points Gauss-Laguerre quadrature for the region $(0, 1)$ and $(1, \infty)$ were used. For $\eta = 0$, which corresponds to the quarter plane problem, Mellin transforms were used to calculate the stress components.

The case that the quarter space is subjected to a concentrated normal loading was considered in some detail by Hetényi[1], using a method which is equivalent to solving the integral equations (11) and (12) by an iterative scheme (reflection). The free surface is divided into small rectangles where each element of the integration scheme was based upon Love's solution[9] for the elastic half space subjected to a uniformly distributed normal load over a rectangle. Figures 2 show a comparison of the computed stress components (solid line) with Hetényi's (point values). Results by both methods match well except for the case when $\nu = 0$,

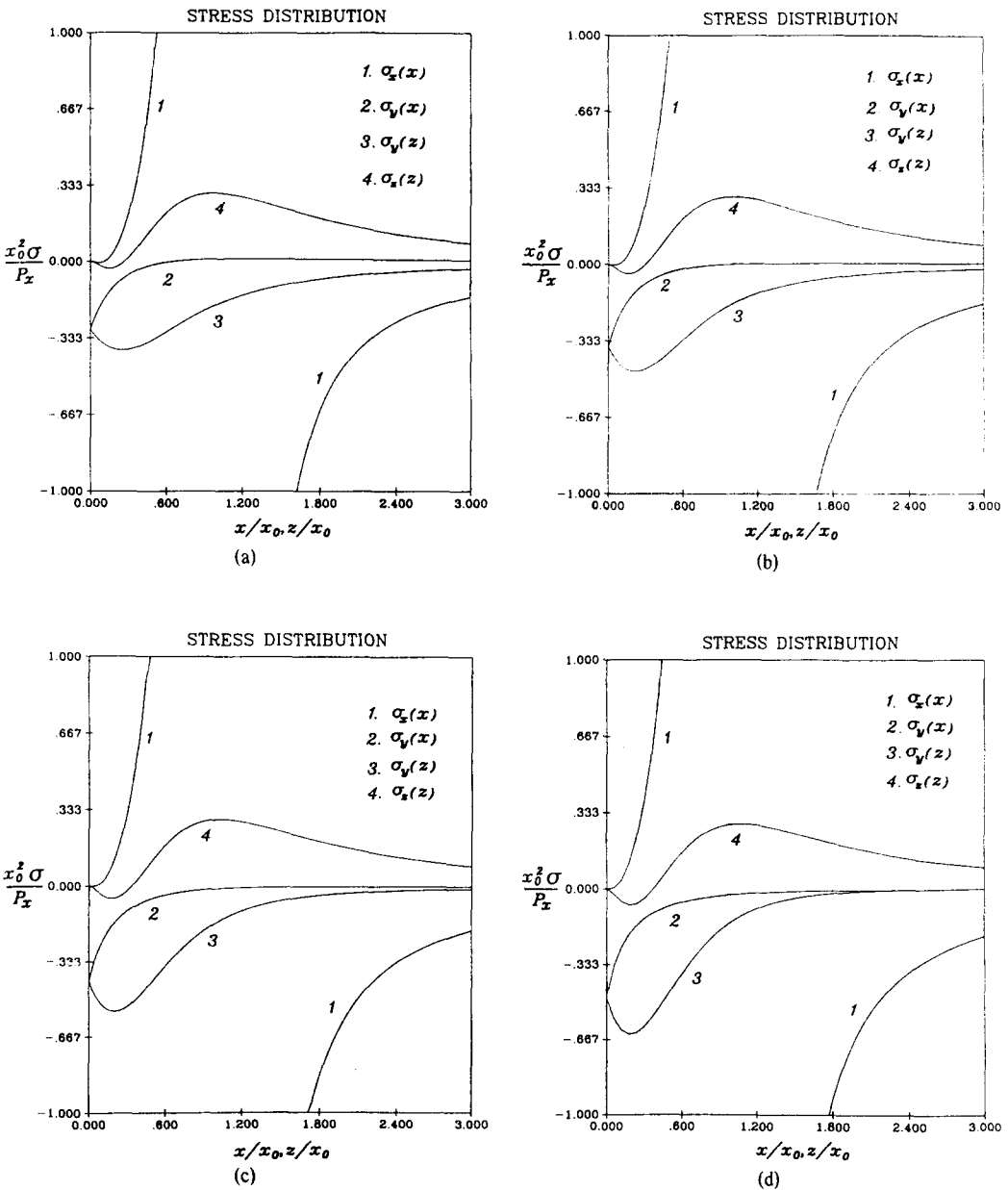


Fig. 3. Stress distributions along the crest ($y = 0$) for the quarter space under tangential loading perpendicular to the edge (a) $\nu = 0$; (b) $\nu = 1/6$; (c) $\nu = 1/3$; (d) $\nu = 1/2$.

Table 1. Displacement fields along the crest ($y = 0$) for the quarter space under normal loading

x	0	0.0690	0.1270	0.2939	0.5358	0.8865	1.1281	1.4415	2.4737	3.4026	
$v = 0$	$\frac{\mu u_x x_0}{p_z}$	0	0.0002	0.0012	0.0129	0.0660	0.5973	-0.7211	-0.2735	-0.1278	-0.0941
	$\frac{\mu u_z x_0}{p_z}$	0	0.0134	0.0245	0.0610	0.1627	1.1993	1.0271	0.1309	-0.1505	-0.2065
$v = \frac{1}{6}$	$\frac{\mu u_x x_0}{p_z}$	0	0.0012	0.0029	0.0136	0.0537	0.4144	-0.4604	-0.1576	-0.0497	-0.0213
	$\frac{\mu u_z x_0}{p_z}$	0	0.0097	0.0177	0.0454	0.1272	0.9881	0.8432	0.0950	-0.1423	-0.1904
$v = \frac{1}{3}$	$\frac{\mu u_x x_0}{p_z}$	0	0.0011	0.0025	0.0104	0.0356	0.2243	-0.2078	-0.0502	0.0186	0.0414
	$\frac{\mu u_z x_0}{p_z}$	0	0.0053	0.0098	0.0273	0.0877	0.7712	0.6527	0.0515	-0.1436	-0.1847
$v = \frac{1}{2}$	$\frac{\mu u_x x_0}{p_z}$	0	0.0002	0.0008	0.0046	0.0140	0.0295	0.0398	0.0517	0.0808	0.0976
	$\frac{\mu u_z x_0}{p_z}$	0	0.0003	0.0009	0.0070	1.0447	0.5497	0.4570	0.0022	-0.1520	-0.1867

z	0	0.0690	0.1270	0.2939	0.5358	0.8865	1.1281	1.4415	2.4737	3.4026	
$v = 0$	$\frac{\mu u_x x_0}{p_z}$	0	-0.0137	-0.0256	-0.0581	-0.0874	-0.0909	-0.0807	-0.0649	-0.0304	-0.0172
	$\frac{\mu u_z x_0}{p_z}$	0	0	0.0003	0.0039	0.0110	0.0067	-0.0073	-0.0320	-0.1089	-0.1515
$v = \frac{1}{6}$	$\frac{\mu u_x x_0}{p_z}$	0	-0.0097	-0.0182	-0.0406	-0.582	-0.0524	-0.0389	-0.0206	0.0189	0.0351
	$\frac{\mu u_z x_0}{p_z}$	0	0.0011	0.0021	0.0066	0.0134	0.0089	-0.0040	-0.0264	-0.0960	-0.1376
$v = \frac{1}{3}$	$\frac{\mu u_x x_0}{p_z}$	0	-0.0053	-0.100	-0.0223	-0.0290	-0.0156	0	0.0197	0.0616	0.0796
	$\frac{\mu u_z x_0}{p_z}$	0	0.0008	0.0015	0.0044	0.0079	0.0010	-0.0117	-0.0326	-0.0958	-0.1335
$v = \frac{1}{2}$	$\frac{\mu u_x x_0}{p_z}$	0	-0.0003	-0.0009	-0.0028	0.0010	0.0209	0.0378	0.0579	0.1004	0.1193
	$\frac{\mu u_z x_0}{p_z}$	0	-0.0003	-0.0007	-0.0014	-0.0031	-0.0143	-0.0276	-0.0475	-0.1050	-0.1390

Table 2. Displacement fields along the crest ($y = 0$) for the quarter space under tangential loading perpendicular to the edge

x	0	0.0690	0.1270	0.2939	0.5358	0.8865	1.1281	1.4415	2.4737	3.4026	
$v = 0$	$\frac{\mu u_x x_0}{p_x}$	0	-0.0001	-0.0002	0.0065	0.0722	1.0695	0.8769	-0.0402	-0.3642	-0.4414
	$\frac{\mu u_z x_0}{p_x}$	0	0.0148	0.0265	0.0502	0.0407	-0.4433	0.8996	0.4772	0.3826	0.3743
$v = \frac{1}{6}$	$\frac{\mu u_x x_0}{p_x}$	0	0.0014	0.0025	0.0120	0.0814	1.0829	0.8925	-0.0223	-0.3416	-0.4164
	$\frac{\mu u_z x_0}{p_x}$	0	0.0180	0.0323	0.0641	0.0750	-0.2313	0.6716	0.3973	0.3477	0.3481
$v = \frac{1}{3}$	$\frac{\mu u_x x_0}{p_x}$	0	0.0030	0.0051	0.0174	0.0901	1.0954	0.9070	-0.0056	-0.3205	-0.3932
	$\frac{\mu u_z x_0}{p_x}$	0	0.0714	0.0384	0.0786	0.1098	-0.0190	0.4438	0.3173	0.3119	0.3207
$v = \frac{1}{2}$	$\frac{\mu u_x x_0}{p_x}$	0	0.0046	0.0077	0.0226	0.0984	1.1073	0.9209	0.0102	-0.3005	-0.3710
	$\frac{\mu u_z x_0}{p_x}$	0	0.0251	0.0449	0.0936	0.1451	0.1935	0.2160	0.2372	0.2754	0.2921

z	0	0.0690	0.1270	0.2939	0.5358	0.8865	1.1281	1.4415	2.4737	3.4026	
$v = 0$	$\frac{\mu u_x x_0}{p_x}$	0	-0.0148	-0.0279	-0.0471	-0.1591	-0.2777	-0.3404	-0.3997	-0.4972	-0.5342
	$\frac{\mu u_z x_0}{p_x}$	0	-0.0002	-0.0009	-0.0022	0.0093	0.0533	0.0893	0.1316	0.2206	0.2606
$v = \frac{1}{6}$	$\frac{\mu u_x x_0}{p_x}$	0	-0.0179	-0.0330	-0.0819	-0.1640	-0.2739	-0.3313	-0.3854	-0.4746	-0.5086
	$\frac{\mu u_z x_0}{p_x}$	0	0.0017	0.0028	0.0064	0.0220	0.0658	0.0995	0.1388	0.2211	0.2585
$v = \frac{1}{3}$	$\frac{\mu u_x x_0}{p_x}$	0	-0.0211	-0.0384	-0.0899	-0.1688	-0.2694	-0.3213	-0.3701	-0.4514	-0.4829
	$\frac{\mu u_z x_0}{p_x}$	0	0.0037	0.0067	0.0155	0.0352	0.0782	0.1095	0.1452	0.2199	0.2541
$v = \frac{1}{2}$	$\frac{\mu u_x x_0}{p_x}$	0	-0.0247	-0.0442	-0.0982	-0.1736	-0.2644	-0.3106	-0.3541	-0.4276	-0.4568
	$\frac{\mu u_z x_0}{p_x}$	0	0.0059	0.0109	0.0250	0.0490	0.0909	0.1193	0.1511	0.2174	0.2481

which among the values of Poisson's ratios produces the largest magnitude of singularity. For small values of x or z the components of σ_x and σ_z do not match well. For Poisson's ratio differing from $1/2$ the normal stresses at the crest on the top surface become infinitely large as $1/r^2$ where r is the distance from the loading point to the evaluated point; this represents the contribution from the concentrated loading. From Boussinesq's solution for the half space we recognize that the magnitude of the singularity is proportional to $(1 - 2\nu)/2\pi x_0^2$. Also presented are the displacement fields corresponding to these various x values of Poisson's ratio. Gerber[3] followed Hetényi's method to solve the related punch problem for the quarter space but was restricted, since the punch could not approach close to the edge. The rectangles, in the algorithm, had equal spacing in the y -direction but different spacings in the x or z direction. Shah and Kobayashi[10] successfully used Love's solution to remove the residual normal stress on the free surface which was divided into 175 small squares. Sizes of these squares were selected such that the variations of the surface tractions with the size of the square did not exceed maximum values.

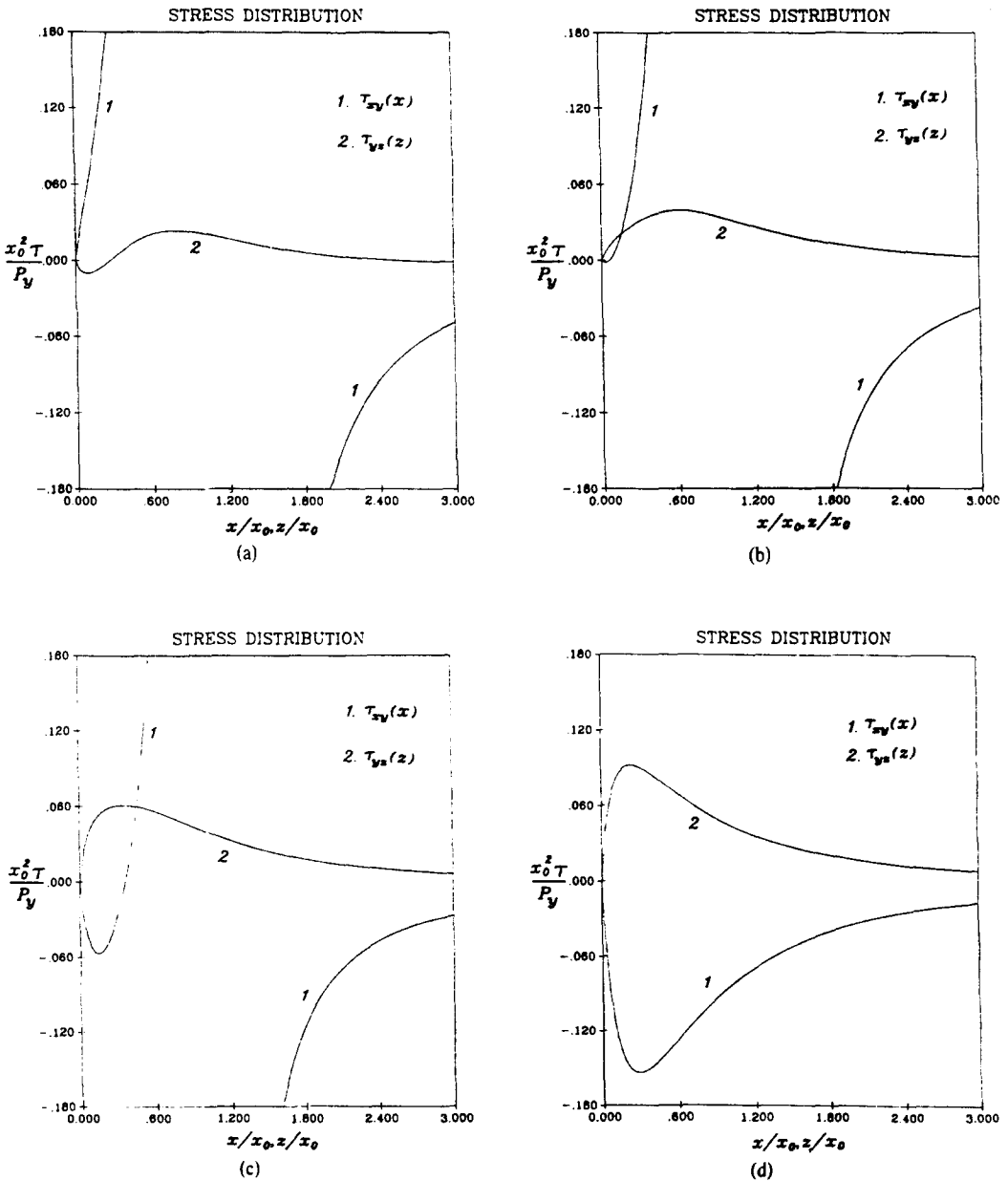


Fig. 4. Stress distributions along the crest ($y = 0$) for the quarter space under tangential loading parallel to the edge (a) $\nu = 0$; (b) $\nu = 1/6$; (c) $\nu = 1/3$; (d) $\nu = 1/2$.

Table 3. Displacement fields along the crest ($y = 0$) for the quarter space under tangential loading parallel to the edge

x	0	0.0690	0.1270	0.2939	0.5358	0.8865	1.1281	1.4415	2.4737	3.4026	
$v = 0$	$\mu u_y x_0 / P_y$	0	0.0044	0.0101	0.0384	0.1378	1.1768	1.0071	0.1139	-0.1607	-0.2134
$v = \frac{1}{6}$	$\mu u_y x_0 / P_y$	0	0.0087	0.0162	0.0443	0.1294	0.9958	0.8543	0.1097	-0.1199	-0.1642
$v = \frac{1}{3}$	$\mu u_y x_0 / P_y$	0	0.0120	0.0206	0.0466	0.1156	0.8075	0.6932	0.0962	-0.0904	-0.1272
$v = \frac{1}{2}$	$\mu u_y x_0 / P_y$	0	0.0147	0.0240	0.0466	0.0979	0.6140	0.5262	0.0762	-0.0687	-0.0987

z	0	0.0690	0.1270	0.2939	0.5358	0.8865	1.1281	1.4415	2.4737	3.4026	
$v = 0$	$\mu u_y x_0 / P_y$	0	-0.0112	-0.0208	-0.0477	-0.0829	-0.1239	-0.1459	-0.1688	-0.2156	-0.2386
$v = \frac{1}{6}$	$\mu u_y x_0 / P_y$	0	-0.0094	-0.0169	-0.0371	-0.0634	-0.0953	-0.1130	-0.1314	-0.1694	-0.1879
$v = \frac{1}{3}$	$\mu u_y x_0 / P_y$	0	-0.0087	-0.0147	-0.0294	-0.0487	-0.0734	-0.0877	-0.1029	-0.1342	-0.1694
$v = \frac{1}{2}$	$\mu u_y x_0 / P_y$	0	-0.0087	-0.0136	-0.0239	-0.0371	-0.0561	-0.0678	-0.0805	-0.1069	-0.1194

The preceding are some of the examples that use Love's solution to treat the quarter space problem. If the surface traction is large or even singular, this approach may not be good enough. For the case that the quarter space is subjected to tangential loading P_x , the magnitude of the singularity is quite large. If Love's solution based on Shah and Kobayashi's criterion is used without removing the singular part, the number of rectangles required would exceed the computer storage. On the other hand if the singular part was removed using the modified Bessel function $K_0(s)$, as suggested here, the new loading would oscillate and a relatively large number of rectangles would still be required to make the results sufficiently accurate.

The remainder of the results are given in Fig. 3 and Table 2, which show the stress and displacement distributions along the crest for the quarter space under tangential loading perpendicular to the edge, and Fig. 4 and Table 3, which show the stress and displacement distributions along the crest for the quarter space under tangential loading parallel to the edge.

Acknowledgement—The authors are grateful for support from the National Science Foundation grant CME 7918015.

REFERENCES

1. M. Hetényi, A general solution for the elastic quarter space. *J. Appl. Mech.* 37, *Trans. ASME, Series E*, 70 (1970).
2. M. Hetényi, A method of solution for the elastic quarter plane. *J. Appl. Mech.* 27, *Trans. ASME* 82, Series E, No. 2, 289–296 (1960).
3. C. E. Gerber, *Contact problems for the elastic quarter plane and for the quarter space*. Doctoral Dissertation, Stanford University, 1968.
4. V. D. Kupradze *et al.*, *Three-dimensional Problems of the Mathematical Theory of Elasticity and Thermoelasticity*. North-Holland, Amsterdam (1979).
5. M. E. Gurtin, Linear theory of elasticity. In *Handbuch der Physik* (Edited by S. Flügge), Vol. VI a/2, p. 147. Springer-Verlag, Berlin (1972).
6. I. N. Sneddon, Fourier transform solution of quarter plane problems in elasticity. File No. PSR-9916, Applied Mathematics Research Group, North Carolina State University, 1971.
7. J. Dunders and M.-S. Lee, Stress concentration at a sharp edge in contact problem. *J. Elasticity* 2, 109–112 (1972).
8. C. T. H. Baker, *The Numerical Treatment of Integral Equations*. Clarendon Press, Oxford (1977).
9. A. E. H. Love, The stress produced in a semi-infinite solid by pressure on part of the boundary. *Philosophical Trans. Royal Soc., London, Series A* 228, 377–420 (1929).
10. R. C. Shah and A. S. Kobayashi, On the surface flaw problem. *The Surface Crack; Physical Problems and Computational Solution*, ASME Special Volume, pp. 79–124 (1972).